

# Superconducting energy gap distribution of MgB<sub>2</sub> investigated by point-contact spectroscopy

F. Laube<sup>1</sup>, G. Goll<sup>1</sup>, J. Hagel<sup>1</sup>, H. v. Löhneysen<sup>1,2</sup>, D. Ernst<sup>2</sup>, T. Wolf<sup>2</sup>

<sup>1</sup>Physikalisches Institut, Universität Karlsruhe, D-76128 Karlsruhe, Germany

<sup>2</sup>Forschungszentrum Karlsruhe, Institut für Festkörperphysik, D-76021 Karlsruhe, Germany  
(April 26, 2024)

We performed point-contact spectroscopy on the binary superconductor MgB<sub>2</sub>. The differential conductance shows gap-related structures which vary in width and position from contact to contact. The distribution of energy gaps shows a distinct accumulation around 1.7 and 7 meV which is associated with the occurrence of a small and a large energy gap in MgB<sub>2</sub>. While with increasing  $T$  the structure in  $dI/dV$  associated with the small gap is present up to  $T_c$ , in magnetic field it is suppressed well below  $B_{c2}$ .

PACS numbers: 74.70.Ad, 74.80.Fp, 74.20.Rp

The observation of superconductivity at 39 K in the simple binary compound MgB<sub>2</sub> [1] was a surprise for most condensed matter scientists and immediately raises the question of the mechanism of superconductivity in this material. Following a basic approach to superconductivity, two key issues have to be considered: the order-parameter symmetry and the coupling mechanism. For the latter, a significant boron isotope effect was observed in MgB<sub>2</sub> [2] which is consistent with a phonon-mediated BCS mechanism where the boron phonon modes are playing an important role. A moderately strong electron-phonon coupling constant  $\lambda_{el-ph} \approx 0.8$  was derived from measurements of the specific heat [3] in good agreement with recent theoretical predictions [4–6].

The order-parameter symmetry has already been investigated by tunneling spectroscopy and point-contact spectroscopy (PCS) [7–15]. Although the spectra show unambiguous features of an energy gap in the density of states, probably with  $s$ -wave symmetry of the order parameter, the results are controversial on the gap width. Values of  $2\Delta/k_B T_c$  ranging from 1.2 to 4.7 have been reported, raising the possibility of an anisotropic energy gap or even multiple gaps. Careful analysis of specific-heat measurements [16,17] and photoemission spectroscopy [18] support this scenario as well.

We present measurements of the differential conductance  $dI/dV$  of normal conductor/superconductor point contacts between a Pt tip and a MgB<sub>2</sub> pellet. The MgB<sub>2</sub> pellet was prepared in an Ar atmosphere from magnesium filings (> 99.9%, Chempure) and powdered boron (99%, Ventron). The powders were mixed in the ratio Mg:B = 1.1:2 and pressed into a pellet. After wrapping the pellet in a Ta foil it was enclosed in an Fe cylinder and inserted in a high-pressure furnace. The pellet was then heated to 1073 K for 1.5 h and to 953 K for 2 h under an Ar pressure of 58 MPa. The DC magnetization of the pellet (Fig. 1) indicates an onset superconducting transition temperature  $T_c^{onset} = 38.2$  K. Almost the full

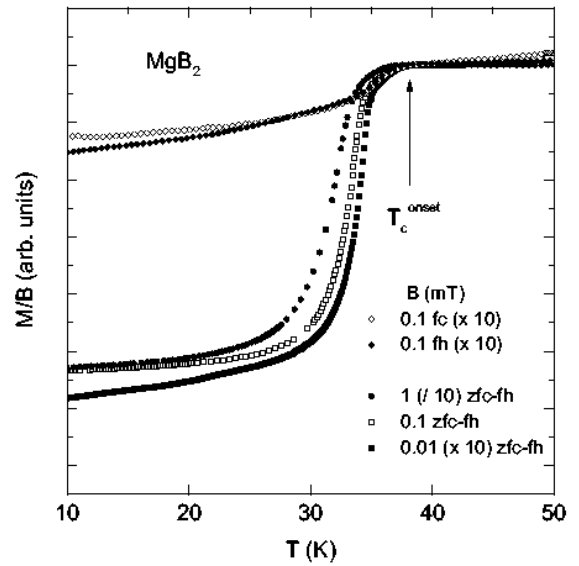


FIG. 1. DC magnetization of MgB<sub>2</sub> in different applied magnetic fields.

theoretical shielding signal is reached in 1 mT applied field in a zero-field cooled (zfc) – field heated (fh) temperature cycle. The Meissner signal remains weak, i. e. of the order of a few percent. Upon reducing the applied field to 10  $\mu$ T, a kink in the transition curve at 35 K reveals the granular structure of the sample: below  $T_c^{onset}$  first the individual grains become superconducting, below 35 K intergranular shielding currents cause shielding of the whole pellet.

PCS spectra were taken on as grown and polished surfaces of the MgB<sub>2</sub> pellet. Different contacts were established in situ at low temperatures in liquid Helium. The PCS spectra, i. e. the differential resistance  $dV/dI$  vs  $V$  were obtained using a standard four-point lock-in technique. The zero-bias resistance  $R_0$  of stable contacts ranges from 1 to 60  $\Omega$ .  $dI/dV$  vs  $V$  curves are obtained by numerical inversion of the  $dV/dI$  data. The  $dI/dV$

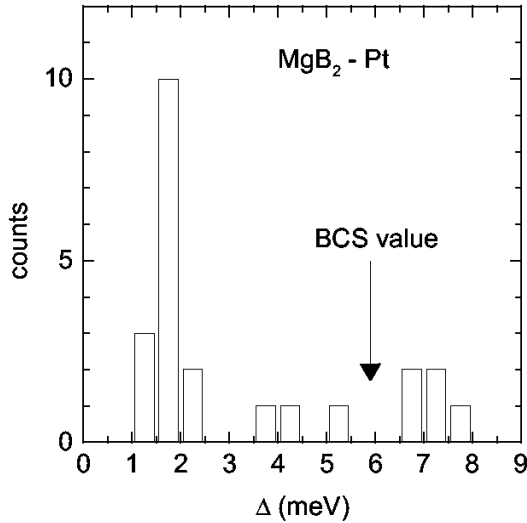


FIG. 2. Extracted values of the gap energy for different  $\text{MgB}_2$  contacts

curves taken at low  $T \ll T_c$  (between 1.7 and 5 K, cf. Fig. 3), show most often maxima at voltage  $\pm V_0$ , presumably related to the superconducting energy gap  $\Delta$ . The position of the maxima  $\Delta = eV_0$ , varies depending on the location of the Pt needle on the polycrystalline sample where the point contact was established. The histogram depicted in Fig. 2 summarizes the position of maxima of 20 contacts. In a few cases a single maximum centered at  $V = 0$  was observed (Fig. 3e). For these cases the value of  $\Delta_0 = \Delta(T \rightarrow 0)$  was derived from the modified BTK fit (see below) and is also included in Fig. 2. This histogram in nice consistency reflects the gap distribution reported in literature. One dominant feature is a maximum at about 1.7 meV, a second occurs at about 7 meV.

Following the BTK theory [20] of transport through a metallic microcontact between a normal metal (N) and an isotropic superconductor (S), Andreev reflection is the dominant transport process at the N-S interface. Andreev-reflected charge carriers lead to an excess current which increases the point-contact conductance. Depending on the strength of the interface barrier a characteristic double-maximum feature is expected in  $dI/dV$ , with the maxima at  $\pm\Delta/e$  where  $\Delta$  is the energy gap. Inelastic scattering in the contact region usually leads to a smearing and weakening of the gap-related features. This can be empirically taken into account by replacing the quasiparticle energy  $E$  with  $E + i\Gamma$ , where  $\Gamma$  parametrizes the finite lifetime of the quasiparticles [19]. We observed a few contacts where the  $dI/dV$  curves show maxima at  $\pm V_0$  and  $\pm V_1$ . These curves can be regarded as a superposition of two double-maximum features. Consequently, the maxima are interpreted as being associated with two different energy gaps and the presence of multigap super-

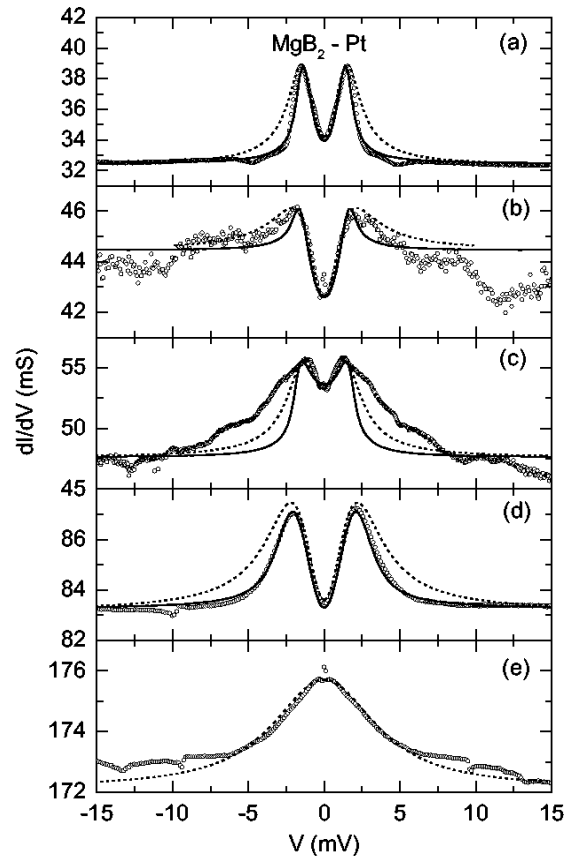


FIG. 3. Measured  $dI/dV$  curves and BTK fits to the small gap structures for different  $\text{MgB}_2/\text{Pt}$  contacts at  $T = 1.7$  K (panel a-c) and 5 K (panel d and e) either with thermal smearing only ( $\Gamma = 0$ , solid lines) or with additional finite-lifetime smearing ( $\Gamma \neq 0$ , dashed lines). The fit parameters are summarized in Table I.

conductivity in  $\text{MgB}_2$ .

Multigap superconductivity in  $\text{MgB}_2$  has recently theoretically been suggested by Liu *et al.* [4] based on the electronic structure proposed by Kortus *et al.* [21]: The Fermi surface consists of two sets of sheets, two-dimensional (2D) cylindrical sheets and three-dimensional (3D) tubular network. In the clean limit, two different superconducting order parameter are predicted: a larger one on the 2D part of the Fermi surface, a smaller one (about 1/3) on the 3D part of the Fermi surface. The multi-sheetedness of the Fermi surface should lead to a substantial difference between the in-plane and out-of-plane tunneling spectra. The effect of strong defect scattering drives the system into the dirty limit where the two energy gaps are mixed and an isotropic BCS gap is obtained. Quite remarkable is the effect on the temperature dependence of the gap in both limits. In the clean limit both energy gaps close at  $T_c$  while in the dirty limit the resultant isotropic gap is substantially suppressed.

In the following we focus on spectra which show

	solid lines				dashed lines		
	$T$ (K)	$\Delta_0$ (meV)	$Z$	$r$	$\Delta_0$ (meV)	$\Gamma$ (meV)	$Z$
(a)	1.7	1.5	0.5	0.368	1.5	0.65	0.57
(b)	1.7	1.7	0.8	0.079	1.1	1.4	0.9
(c)	1.7	1.7	0.3	0.305	1.5	0.87	0.47
(d)	5	2.1	0.615	0.128	1.3	1.3	0.73
(e)	5	–	–	–	1.1	3.6	0.1

TABLE I. Fit parameter of the theoretical curves in Fig. 3

features associated with the small gap structure only. Fig. 3a-e show a number of spectra of this type together with theoretical curves calculated within the modified BTK theory either with thermal smearing only ( $\Gamma = 0$ , solid lines) or with additional finite-lifetime smearing ( $\Gamma \neq 0$ , dashed lines). The fit parameters of these curves are summarized in Table I. Although the width of the spectra is almost the same, the voltage dependence is different. Curve a and d (referred to as type 1) are described very well with a pure ( $\Gamma = 0$ ) BTK fit with an energy gap (assumed to be isotropic)  $\Delta_0 = 1.5$  meV (a) and  $\Delta_0 = 2.1$  meV (d), a barrier strength  $Z = 0.5$  (a) and  $Z = 0.615$  (d), respectively. The fits have been scaled by a factor of  $r = [dI/dV(0) - dI/dV(15 \text{ mV})]_{\text{exp}}/[dI/dV(0) - dI/dV(15 \text{ mV})]_{\text{theo}} = 0.368$  (a) and  $0.128$  (d), respectively, in order to meet the absolute magnitude of the experimental conductance change  $[dI/dV(0) - dI/dV(15 \text{ mV})]_{\text{exp}}$ . The common feature of curve b, c, and e (referred to as type 2) is that the decrease of the conductance for  $V \geq \Delta/e$  is weaker than expected from a pure BTK fit, i. e. the experimental curves are much wider. Smearing due to inelastic scattering in the contact region can be one origin of wider structures which has been modelled by  $\Gamma \neq 0$ . The parameters  $\Delta$ ,  $\Gamma$ , and  $Z$  are chosen in such a way that the calculated curves describe the experimental conductance change without the necessity of scaling. Introducing of  $r$  as an additional fit parameter to improve the fit would require an unphysical value  $r > 1$ . A relatively large  $\Gamma$  of the same order of magnitude as  $\Delta$  or even larger is needed to model the curves, and the resulting description of the spectra is not really satisfactory. The failure of the model in describing curve c hints at a second, intrinsic origin, namely an apparent gap distribution due to an anisotropic small gap. This means that in addition to the occurrence of two energy gaps in  $\text{MgB}_2$ , these gaps themselves might not be isotropic. Recently Giubileo *et al.* [14] pointed out that the gap width varies even in the case where spatial inhomogeneities can be ruled out as an origin of a gap distribution. It might be of interest to note that all three curves show a weak conductance maximum around zero-bias which might be caused by nodes of the gap function [12].

In order to further elucidate the difference of the spectra we now turn to the temperature dependence of both

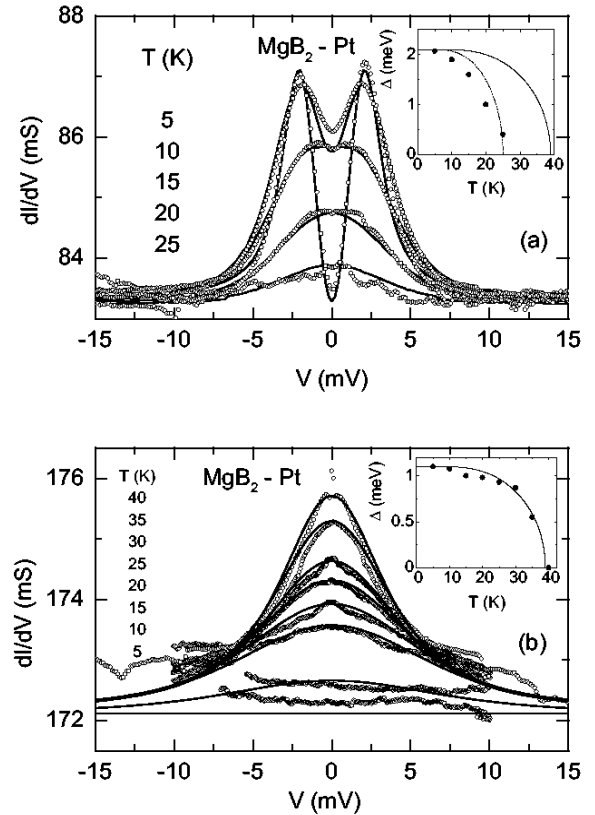


FIG. 4. Temperature dependence of point contacts of type 1 (a) and 2 (b).

types depicted in Fig. 4 a and b together with theoretical curves. With increasing temperature the gap-related structure weakens in both cases. However, while gap-related features of the spectra of type 2 vanish close to the bulk  $T_c$  and almost follow the BCS weak-coupling behavior of  $\Delta(T)$ , the isotropic gap extracted from spectra of type 1 closes at  $\approx 0.7 T_c$ . Without overrating the experimental facts, the results resemble the proposed multi-gap scenario. Bearing in mind the granular structure of the sample and the unknown microscopic structure of the point contact, it is conceivable that both clean and dirty limits are locally realized on different parts of the sample.

In an applied magnetic field  $B$  the gap structure weakens with increasing field and vanishes around 6 T (see Fig. 5). The small gap is much more sensitive to an applied field than expected from estimates of the upper critical field  $B_{c2}(0)$  from resistivity [22] and magnetization measurements [23]. These data suggest that a field well above 12 T is necessary to suppress superconductivity at 1.7 K. Szabo *et al.* have recently reported an even stronger field dependence of the small gap [15]. In line with specific-heat measurements [16,17],  $B = 1$  T substantially suppresses the small gap. The result hints at a different nature of the two energy gaps probably due to their different dimensionality.

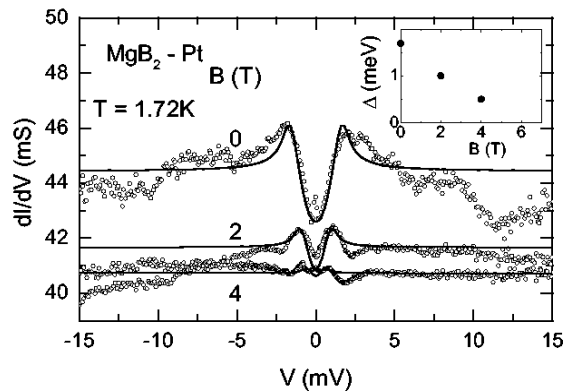


FIG. 5. Magnetic field dependence of the point contact shown in Fig. 3b. The inset shows  $\Delta(B)$  extracted from the BTK fit to the data.

In conclusion, we have examined point contacts on  $\text{MgB}_2$  in order to investigate the superconducting energy gap. The gap width obtained from  $dI/dV$  vs  $V$  spectra varies from contact to contact depending on the microscopic structure and grain orientation in the point-contact region. The result is compatible with multigap superconductivity with a small gap present up to  $T_c$ .

---

[1] J. Nagamatsu, N. Nakagawa, T. Muranaka, Y. Zenitani, J. Akimitsu, *Nature* **410**, 63 (2001).  
[2] S. L. Budko, G. Lapershot, C. Petrovic, C. E. Cunningham, N. Anderson, P. C. Canfield, *Phys. Rev. Lett.* **86**, 1877 (2001).  
[3] R. K. Kremer, B. J. Gibson, and K. Ahn, *cond-mat/0102432v2*.  
[4] A. Y. Liu, J. J. Mazin, and J. Kortus, *cond-mat/0103570*.  
[5] Y. Kong, O. V. Dolgov, O. Jepsen, and O. K. Andersen, *Phys. Rev. B* **64**, 020501(R) (2001).  
[6] K.-P. Bohnen, R. Heid, and B. Renker, *Phys. Rev. Lett.* **86**, 5771 (2001).  
[7] Y. Bugoslavsky, G. K. Perkins, X. Qi, L. F. Coheb, A. D. Caplin, *Nature* **410**, 563 (2001).  
[8] G. Rubio-Bollinger, H. Suderow, S. Vieira, *Phys. Rev. Lett.* **86**, 5582 (2001).  
[9] G. Karapetrov, M. Javarone, W. K. Kwok, G. W. Crabtree, D. G. Hinks, *Phys. Rev. Lett.* **86**, 4374 (2001).  
[10] A. Sharoni, I. Felner, D. Millo, *Phys. Rev. B* **63**, 220508R (2001).  
[11] H. Schmidt, J. F. Zasadzinski, K. E. Gray, D. G. Hinks, *cond-mat/0102389*.  
[12] C.-T. Chen, P. Seneov, N.-C. Yeh, R. P. Vasquez, C. U. Jung, M.-S. Park, H.-J. Kim, W.N. Kang, S.-I. Lee, *cond-mat/0104285*.  
[13] A. Plecenik, Š. Beňačka, P. Kúš, *cond-mat/0104038v2*.  
[14] F. Giubileo, D. Roditcheo, W. Sachs, R. Launy, J. Klein, *cond-mat/0105146*.

[15] P. Szabó, P. Samuely, J. Kacmarčík, Th. Klein, J. Marcus, D. Furchart, S. Miragila, C. Marcenat, A. G. M. Jansen, *cond-mat/0105598*.  
[16] H. D. Yang, J.-Y. Liu, H. H. Li, F. H. Hsu, C. J. Liu, and Changqi Jin, *cond-mat/0104574*.  
[17] F. Bouquet, R. A. Fisher, N. E. Phillips, D. G. Hinks, and J. D. Jorgensen, *cond-mat/0104206*.  
[18] S. Tsuda, T. Yokoya, T. Kiss, Y. Takano, K. Togano, H. Kitou, H. Ihara, and S. Shin, *cond-mat/0104489*.  
[19] R. C. Dynes, V. Naraynamurti, J.P. Garno, *Phys. Rev. Lett.* **41**, 1509 (1978).  
[20] G.E. Blonder, M. Tinkham, T. M. Klapwijk, *Phys. Rev. B* **25**, 4515 (1982).  
[21] J. Kortus, I. I. Mazin, K. D. Belashchenko, V. P. Antropov, L. L. Boyer, *cond-mat/0101446*.  
[22] D. K. Finnemore, J. E. Ostenson, S. L. Bud'ko, G. Laperot, P. C. Canfield, *cond-mat/0102114*.  
[23] D. C. Larbalestier, L. D. Cooley, M. O. Rikel, A. A. Polyanskii, J. Jiang, S. Patnalk, X. Y. Cai, D. M. Feldmann, A. Gurevich, A. A. Squiteri, M. T. Naus, C. B. Eom, E. E. Hellstrom, R. J. Cava, K. A. Regan, N. Rogado, M. A. Hayward, T. He, J. S. Slusky, P. Khalifah, K. Inumaru, M. Haas, *Nature* **410**, 186 (2001).